FLOOD MAPPING USING SENTINEL-1 SAR DATA: A CASE STUDY OF ORDU 8 AUGUST 2018 FLOOD

[a]B. Tavus *, [a]S. Kocaman, [b]H.A. Nefeslioglu, [b]C. Gokceoglu

[a] Hacettepe University, Dept. of Geomatics Engineering, 06800 Ankara, Türkiye - (beste.tavus, sultankocaman)@hacettepe.edu.tr
[b] Hacettepe University, Dept. of Geological Engineering, 06800 Ankara, Türkiye - (hanefeslioglu, cgokce)@hacettepe.edu.tr

KEY WORDS: Flood Mapping, Sentinel-1, Ordu City, SAR, Classification

ABSTRACT:

Flood events are among the disasters that occur often in a large part of the world and cause great loss of lives and property. The factors such as rapid urbanization, lack of proper infrastructure development, insufficient consideration of environmental and climate effects cause the flood disaster to be more destructive. For such reasons, the production of flood maps is very important in terms of flood modelling, hazard and risk analysis. Satellite optical imagery based flood analysis methods have frequently been used before, during and after floods. However, the collected data is insufficient due to the clouds occurring during and after the rainfall. In recent years, Synthetic Aperture Radar (SAR) sensors, which provides reliable data in all weather conditions and day-night, have been preferred because it eliminates these limitations of optical images. The aim of this study is to investigate the potential for flood mapping with SAR images classified using different supervised classification algorithms. For this purpose, Fatsa, Ünye, and Çaybaşı districts of Ordu have been mapped using Sentinel-1 SAR data acquired on August 8th, 2018. Sentinel-1A / B SAR images of the study area have been obtained from the European Space Agency (ESA). Pre-processing steps, which consist of trajectory correction, calibration, speckle filtering and terrain correction, have been applied to the images. The random forest (RF), k-nearest neighbour (KNN) and maximum likelihood (ML), which are supervised classification techniques, have been applied to SAR images to detect the flooded areas and the results are discussed here.

1. INTRODUCTION

Devastating flooding events have recently been frequently observed all around the world. Flooding is a major natural hazard in both rural and urban areas. However, the effects of flood disasters on people and economic factors in urban areas are much more severe and influential than those that occur in rural areas. As with any disaster, it is essential to know their spatial expectance (susceptibility) and temporal characteristics (hazard) in order to take the necessary prevention actions. Establishment of accurate inventories is the first part of the susceptibility mapping as well.

The increasing number of Earth Observation (EO) satellites and new sensor technologies provide vast amount of data that can be effectively used for flood mapping. Mainly two different types of sensors are used for flood mapping and monitoring: passive (optical) and microwave (active). Although optical sensors have been used for flood monitoring for a long time, they cannot provide data during flood events due to cloud cover and also at night. SAR sensors can be preferred to detect and monitor flooding events since they provide data all-weather and also night (Manavalan, 2017). Additionally, they are affected less by atmospheric scattering. Because of these characteristics, SAR data have been increasingly used in flood mapping studies (e.g. Zhang et al., 2018; Tavus et al., 2018; etc).

Sentinel-1 satellite, operated by the Copernicus Program of ESA is consist of two satellite sensors (Sentinel-1A/B) with a repeat cycle of 6 days. Each Sentinel-1 satellite has a C-Band SAR sensor operating with 5.405 GHz. They have 4 operational modes with different extents, polarizations, incidence angles and resolutions: Stripmap (SM), Interferometric Wide Area (IW), Extra Wide (EW) and Wave (Cazals et al. 2016). By default, they provide data in IW mode that dual polarized SAR data with VV and VH polarization (Torres et al. 2012).

The main purpose of this study is to map the extents of a flood event, which occurred on August 8th, 2018, in Ordu Province of Turkey using Sentinel-1 data. For this purpose, two different Sentinel-1 datasets have been obtained from the Copernicus Open Access Hub of ESA and pre-processed using the freely provided SNAP Tool for radiometric and geometric calibration and noise filtering. Finally, three different supervised classification techniques RF (random forest), KNN (k-nearest neighbour) and ML (maximum likelihood) have been used as classifiers to detect flooded areas.

2. THE STUDY AREA AND THE DATA

2.1 Study Area

The study area includes in Fatsa and Unye districts of Ordu Province in the northern part of Turkey, in Black Sea Region

* Corresponding author.

(North 41°08'56', East 37°25'-03''). Figure 1 shows the study area, the footprints of the Sentinel-1 datasets.

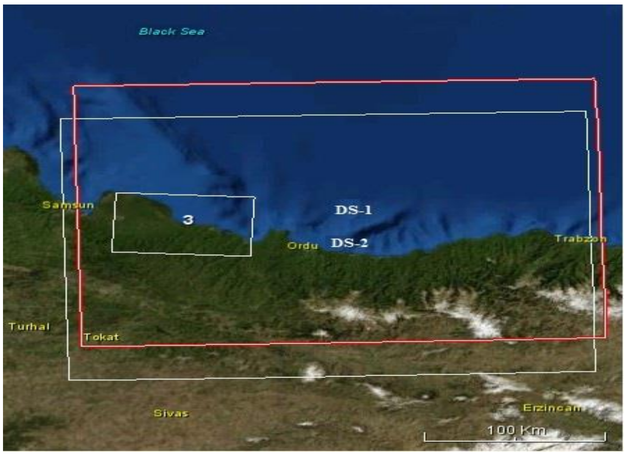

Figure 1. Extents of the SAR data used in the study (DS-1, DS-2) and the sub-area (3) used for flood mapping.

The 60 km long coastal part of Ordu (out of 100 km) consists of sandy beaches, which is a distinctive feature in the Black Sea Region (URL-1). A typical wet Black Sea climate is dominant in Ordu. Almost all months of the year there is precipitation. In addition, there are 36 large and small rivers and streams in Ordu (URL-1). In the province, the most common natural hazard is landslides (80%), followed by floods (9%) and rockfall (8%) based on the data and statistics collected between 1950-2011 (URL-1).

The flood occurred in Ordu on August 8, 2018 caused heavy damages to infrastructure and houses (Figure 2). In total, 8 bridges were destroyed and many landslides have occurred. About 80 kg of precipitation fell to the square meter on Fatsa and Unye Towns and caused stream and river floods. Cevizdere Bridge in Unye Town was demolished due to heavy rain, storm and flood and the Black Sea Coastal Highway was closed to traffic (URL-2).

Figure 2. Examples to damages after Aug 8th, 2018 flood in Ordu (photo credits: https://www.trthaber.com/haber/turkiye/orduda-sel-felaketi-379211.html – accessed on April 10th, 2019).

2.2 Data

In this study, two Sentinel-1 SAR datasets collected in IW mode have been used. Dataset-1 (DS-1) image obtained under the wet weather condition have been used for mapping the flooded areas. In order to delineate the water bodies prior to flooding, another dataset (DS-2) image obtained on July 12th 2018 under the dry weather condition has been used. The main specifications and geographical coverage extents of the SAR datasets used in the study are given in Table 1 and Figure 1, respectively.

ID	Date	Format-Mode	Polarization	Weather
DS-1	10/08/18	GRD-IW	VV + VH	Wet
DS-2	12/0718	GRD-IW	VV + VH	Dry

Table 1. Basic specifications of the Sentinel-1 datasets used in the study.

3. METHODOLOGY

As a first step, a pre-processing has been applied to the SAR images as shown in Figure 3. The pre-processed images have been classified using three well-known supervised classification methods and the classification results have been evaluated to detect the flooded areas. The overall methodological workflow of the study is depicted in Figure 3 and details for each part are given in the following sub-sections.

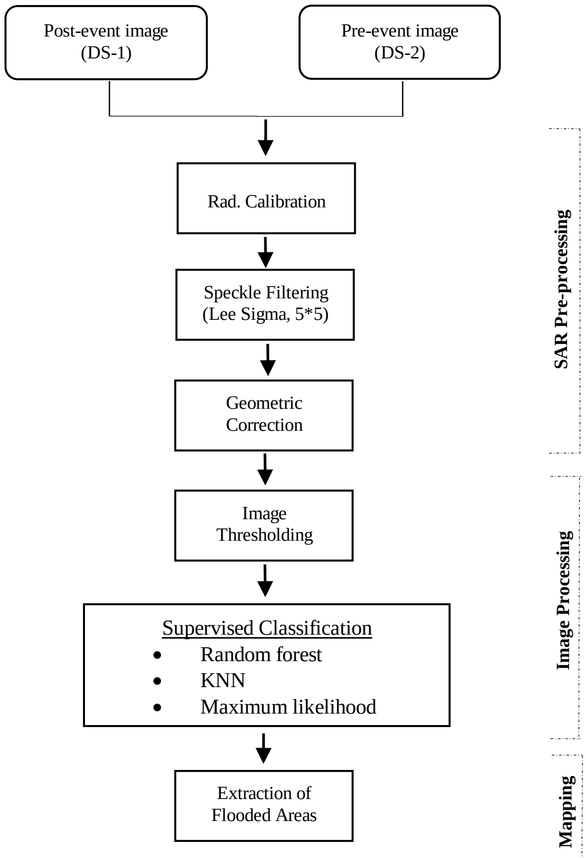

Figure 3. Flowchart of the methodology

3.1 Pre-processing

In order to generate calibrated SAR images, a step-wise procedure with radiometric calibration, speckle filtering and geometric correction have been applied to the SAR datasets. VV polarized images have been preferred because they are considered to be more adequate for flood detection than VH in several previous studies (Psomiadis, 2016; Twele et al. 2016).

First, radiometric calibration has been applied and σ_0 (sigma naught) values have been obtained in dB. The pixels representing water bodies have smaller backscattering coefficient σ_0 compared to other features. Then, Lee Sigma method has been applied to reduce speckle noise effect. Although several other filters (i.e. Boxcar, Lee Sigma and Gamma-MAP) are available in SNAP, the Lee Sigma, has been preferred since it has been reported to supply better results than the others (Lee and Pottier, 2009; Jaybhay and Shastri, 2015; Singh and Shree, 2017).

A geometric correction is needed to remove the effects of side looking geometry of SAR images. At this step, Range Doppler Terrain Correction algorithm has been applied to generate terrain-corrected and orthorectified SAR images. SRTM-3" along with bilinear interpolation have been used as the base digital elevation model (DEM) for the correction.

3.2 Image Classification

Supervised classification is a common approach for information extraction from images and consists of two main stages: training and classification. During the training stage, a set of representative samples are selected for each class and in the classification stage, a classifier is used for the assessment of the probability of every image pixel to belong to the classes. Based on the highest probability, each pixel is classified as a particular feature in the given classification stage.

For this step, histograms of pre-processed images have been used to determine the training sets (Figure 4a,b). The classification has been applied by using three classes (i.e. water bodies, flooded areas and others). The water class show the unchanged (permanent) water areas in both datasets. The same training set has been used for all three classification methods.

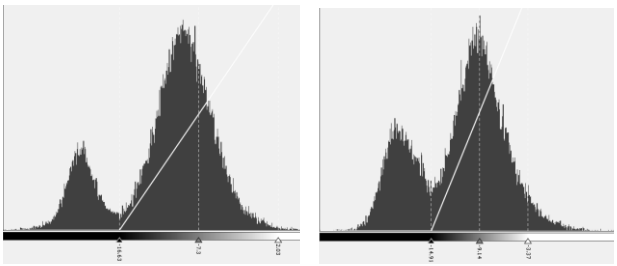

(a) (b)

Figure 4. (a) histogram of pre-event image, (b) histogram of post-event image

The RF classifier samples the data iteratively and randomly and produces a large group of classification and regression trees. The results represent the statistical mode of many decision trees achieving a more robust model than a single classification tree (Breiman, 2011). RF generally supply better classification results than for example the ML method (Van Beijma et al. 2014; Balzter et al. 2015).

The KNN classifies closest training examples in the feature space and it is considered to be a simple machine learning algorithm. In this method, a pixel is assigned to the class amongst its k nearest neighbours (Kanika, 2013). In the ML classification, a pixel with the maximum likelihood is assigned to the corresponding class. In this method, the threshold values for each class are obtained from the training data sets. Depending on the threshold value, the probability of a given pixel for a given class is calculated and all pixels are classified into a specific class (Garga, 2015).

4. RESULTS

The classification results are given in Figure 5. Although the same images and training sets have been used, it has been observed that the classification results are significantly different. The results have been visually assessed using specific regions, including Cuma, Kurna, Elekci Stream and Ilıca Rivers as shown in Figure 6.

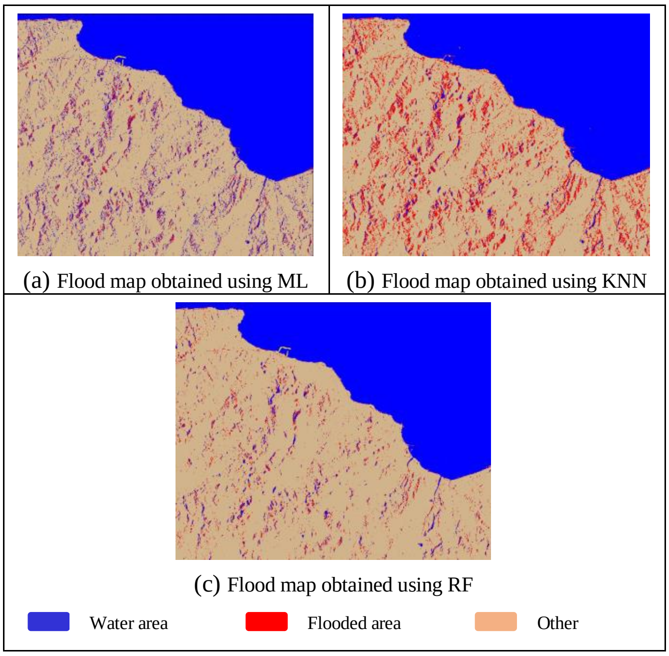

(a) Flood map obtained using ML (b) Flood map obtained using KNN

(c) Flood map obtained using RF

Figure 5. Classification results from different methods

Figure 6. Some of the streams and rivers in the study area (image credit: Google Earth)

In the visual assessment, it could be observed that the results of ML and RF classification generally represent the susceptible flood regions around the streams given in Figure 6. The RF method has provided better results than KNN and ML classifiers. However, the shadow effect in SAR images prevent from the determination of all flooded areas. Especially the KNN method classifies more pixels as flooded. Further investigations are needed with more training data that belongs to flood class. Misclassification of water pixels in three supervised classification results have led to over detection of the flooded areas.

CONCLUSION

In this study, the possibility of determining the flooded areas by classifying Sentinel-1 SAR data acquired over Ordu, Turkey in summer 2018 has been investigated. For this purpose, pre- and post-disaster Sentinel-1 SAR data have been pre-processed and images have been generated using the SNAP Tool. These images have been classified using three well-known classification methods. According to the visual assessments, the RF classifier perform best among all.

Here, no reference data could be used and the methods and the results can be improved using reference data the classification of flood areas. When selecting training data, reference or ground truth data should be used to improve the accuracy. In addition, the layover and foreshortening affects in SAR images have led to misclassification results in some areas. The use of SAR and MS images and higher resolution data could increase the accuracy of the detected floods especially in urban areas.

REFERENCES

Balzter, H., Cole, B., Thiel, C., and Schmullius, C., 2015. Mapping CORINE Land Cover from Sentinel-1A SAR and SRTM Digital Elevation Model Data using Random Forests. *Remote Sensing*, Vol.7, pp. 14876-14898.

Breiman, L. 2001. Random forests. Machine Learning 45, pp. 5-32.

Cazals, C., Rapinel, S., Frison, P.L., Bonis, A., Mercier, G., Mallet, C., Corgne, S., Rudant, J.P., 2016. Mapping and characterization of hydrological dynamics in a coastal marsh using high temporal resolution Sentinel-1A images. *Remote Sensing* 8(7):570 DOI 10.3390/rs8070570.

Garga, P.K 2015. The Role Of Satellite Derived Data For Flood Inundation Mapping Using GIS. *The International Archives of the Photogrammetry, Remote Sensing and Spatial Information Sciences*, Volume XL-3/W3.

Jaybhay, J., Shastri, R., 2015. A study of speckle noise reduction Filters. Signal & Image Processing: An International Journal (SIPIJ), Vol 6, No 3.

Kanika, K., Anil, K,G., Rhythm, G. 2013. A Comparative Study of Supervised Image Classification Algorithm for Satellite Images. *International Journal of Electrical, Electronics and Data Communication*, Vol. 1, Issue 10, pp. 10-16

Lee, J.S., Pottier, E., 2009. Polarimetric Radar Imaging: From basics to applications. In Optical Science and Engineering; CRC Press: Boca Raton, FL, USA, Volume 142.

Manavalan, R. 2017. SAR image analysis techniques for flood area mapping - literature survey. Earth Science Informatics, 10(1), 1–14. https://doi.org/10.1007/s12145-016-0274-2.

Plank, S., 2014. Rapid damage assessment by means of multi-temporal SAR- A comprehensive review and outlook to Sentinel-1. Remote Sensing, Vol 6, pp. 4870–4906, https://doi.org/10.3390/rs6064870.

Psomiadis, E., 2016. Flash flood area mapping utilizing Sentinel-1 radar data. In Proceedings of the Earth Resources and Environmental Remote Sensing/GIS Applications VII, Edinburgh, UK, 26–29 September; doi:10.1117/12.2241055.

Singh, P., Shree, R., 2016. Analysis and effects of speckle noise in SAR images. In Advances in Computing, Communication, & Automation (Fall), ICACCA 2016, pp. 2–6, DOI 10.1109/ICACCAF.2016.7748978.

Tavus, B., Kocaman, S., Nefeslioglu, H., Gokceoglu, C., 2018. Considerations on the Use of Sentinel-1 Data in Flood Mapping in Urban areas: Ankara (Turkey) 2018 Floods. The International Archives of the Photogrammetry, Remote Sensing and Spatial Information Sciences, Volume XLII-5, 2018. ISPRS TC V Mid-term Symposium “Geospatial Technology – Pixel to People”, 20–23 November 2018, Dehradun, India

Torres, R., P. Snoeij, D. Geudtner, D. Bibby, M. Davidson, E. Attema, P. Potin, et al. 2012. “GMES Sentinel-1 Mission.” Remote Sensing of Environment 120: 9–24. doi:10.1016/j.rse.2011.05.028.

Twele, A., Cao, W.X., Plank, S., Martinis, S., 2016. Sentinel-1-based flood mapping: a fully automated processing chain. *International Journal of Remote Sensing*, Vol 37 (13) pp.2990-3004, https://doi.org/10.1080/01431161.2016.1192304.

Van Beijma, S., Comber, A., Lamb, A., 2014. Random forest classification of salt marsh vegetation habitats using quad-polarimetric airborne SAR, elevation and optical RS data. *Remote Sensing Environent*, Vol 149, pp. 118–129, https://doi.org/10.1016/j.rse.2014.04.010.

Zhang, B., Wdowinski, S., Oliver-Cabrera, T., Koirala, R., Jo, M.J., Osmanoglu, B., 2018. Mapping the Extent and Magnitude of Sever Flooding Induced by Hurricane IRMA with MultiTemporal SENTINEL-1 SAR and Insar Observations. ISPRSInternational Archives of the Photogrammetry, Remote Sensing and Spatial Information Sciences, pp. 2237-2244, https://doi.org/10.5194/isprs-archives-XLII-3-2237-2018

URL-1: http://www.dsi.gov.tr/docs/sempozyumlar/9-ordu'da meydana-gelen-sel-ta%C5%9Fk%C4%B1n-su bask%C4%B1n%C4%B1-ve-heyelan olaylar%C4%B1n%C4%B1n-genel-de%C4%9Ferlendirmesi (a-demir)DA0BB13A261E.pdf?sfvrsn=2

URL-2: https://www.trthaber.com/haber/turkiye/orduda-sel-felaketi-379211.html